

Wormholes in Poincarè gauge theory of gravity

Amir Hadi Ziaie*

Research Institute for Astronomy and Astrophysics of Maragha (RIAAM), University
of Maragheh, Maragheh, Iran

August 1, 2022

Abstract

In the present work, we seek for static spherically symmetric solutions representing wormhole configurations in Poincarè gauge theory (PGT). The gravitational sector of the Lagrangian is chosen as a subclass of PGT Lagrangians for which, the spin-0⁺ is the only propagating torsion mode. The spacetime torsion in PGT has a dynamical nature even in the absence of intrinsic angular momentum (spin) of matter, hence, we consider a spin-less matter distribution with an anisotropic energy momentum tensor (EMT) as the supporting source for wormhole structure. A class of zero tidal force wormhole solutions is obtained which can asymptotically be either de-Sitter or anti-de-Sitter, depending on the sign of coupling constants. It is seen that the matter distribution obeys the physical reasonability conditions, i.e., the weak (WEC) and null (NEC) energy conditions either at the throat and throughout the spacetime. We further consider varying equations of state in radial and tangential directions via the definitions $w_r(r) = p_r(r)/\rho(r)$ and $w_t(r) = p_t(r)/\rho(r)$ and study the behavior of state parameters with more care. We observe that our solutions allow for wormhole configurations without the need of exotic matter. Observational features of the wormhole solutions are also discussed utilizing gravitational lensing effects. It is found that the light deflection angle diverges at the throat (which indeed, effectively acts as a photon sphere) and can get zero and negative values depending on the model parameters.

1 Introduction

One of the most fascinating features of general relativity (GR) that has attracted many researchers so far, is the possible existence of hypothetical geometries which have nontrivial topological structure, known as wormholes. The concept of wormhole was firstly introduced by Misner and Wheeler through their pioneering works [1, 2], where these objects were obtained from the coupled equations of electromagnetism and GR and were denoted “geons”, i.e., gravitational-electromagnetic entities [3]. Wheeler considered Reissner-Nordstrom or Kerr wormholes, as objects of the quantum foam¹, which connect different regions of spacetime and operate at the Planck scale. These objects were transformed later into Euclidean wormholes by Hawking [4] and others. However, these Wheeler wormholes were properly understood as non-traversable [5] wormholes², and additionally would, in principle, develop some type of singularity [6]. Despite remarkable efforts made in to understand the concept of geon, the geonlike-wormhole structures seem to have been considered as a mathematical curiosity and after the solutions obtained by Wheeler and Misner, there is a 30-year gap between their original work and

*ah.ziaie@maragheh.ac.ir

¹Smooth spacetime of GR enduring quantum-gravitational fluctuations in topology at the Planck scale.

²Since, such type of wormholes do not allow a two way communication between two regions of the spacetime by a minimal surface called the wormhole throat.

the 1988 Morris-Thorne revival of wormhole physics [7, 8]. The authors investigated this issue via introducing a static spherically symmetric metric and discussed the required conditions for physically meaningful Lorentzian traversable wormholes that allow a traveler to cross between the two spacetime regions at will. However, traversability of a wormhole requires inevitably the violation of null energy condition (NEC). In other words, the matter field providing this geometry is known as exotic matter for which the energy density becomes negative resulting in the violation of NEC [9]. Although the violation of energy conditions is unacceptable from the common viewpoint of physicists, it has been shown that some effects due to quantum field theory, e.g., Casimir effect can allow for such a violation [10]. Also, negative energy densities which are required to support the wormhole configuration may be produced through gravitational squeezing of the vacuum [11], see also [9, 12] for more details. However, it is generally believed that all classical forms of matter obey the standard energy conditions.

Researches on physics of wormholes by Morris, Thorne, and Yurtsever have opened up, in recent years, a new field of study in theoretical physics and several publications have appeared in recent years among which we can quote, traversable wormhole geometries constructed by matter fields with exotic EMT [13], phantom or quintom-type energy [14] and wormholes supported by nonminimal interaction between dark matter and dark energy [15], see [16] for a comprehensive review. However, owing to the problematic nature of exotic matter, many attempts have been made toward minimizing its usage and instead, modifying GR, with the purpose of overcoming the issue of energy conditions within wormhole structures. Much research on wormhole solutions in modified gravity has been done including, Lovelock theories [17], Rastall gravity [18], wormhole solutions in modified gravity with curvature-matter coupling [19], scalar-tensor theory [20], $f(R)$ gravity [21], Einstein-Cartan theory (ECT) [22], Einstein-Gauss-Bonnet [23] and other theories [24].

It is now known that GR is the most successful and accurate gravitational theory at classical level. Its prominent description of the gravitational interaction as a purely manifestation of spacetime geometry along with numerous experimental evidences has exalted it as the backbone of modern theory of gravitational interactions, relativistic cosmology and astrophysics [25]. Even up until today, its basic foundations and further implications are continually being reviewed and examined, as in the case of the recent discovery of gravitational waves from a binary black hole system [26] and the first direct experimental verification of the existence of black holes in the Universe [27]. However, alternative theories as extensions of GR have always attracted much attention due to the deep related principal concepts and open issues still unanswered by GR such as, formulation of a consistent quantum theory of gravity, the problem of cosmological and astrophysical spacetime singularities [28] and the problem of invisible components of gravitating matter, i.e., dark energy and dark matter, see e.g., [29] and references given there. Another important issue that motivates one to seek for possible generalizations of GR is to provide a correct basis for involving intrinsic angular momentum (spin) of gravitating sources and its suitable conservation laws within the gravitational interactions. As we know, the ingredients of macroscopic matter are elementary particles obeying at least locally, the rules of quantum mechanics and special theory of relativity. As a consequence, all elementary particles can be classified via irreducible unitary representations of the Poincaré group and can be labeled by mass m and spin s . Mass is connected with the translational part of the Poincaré group and spin with the rotational part. In the microscopic realm of matter, the spin angular momentum becomes important in characterizing the dynamics of matter. One therefore expects that in analogy to the coupling of energy-momentum to the spacetime metric, spin is coupled to a fundamental attribute of spacetime and plays its own role within the gravitational interactions [30]. However, in standard GR, spin does not couple to any specific geometrical quantity. The simplest generalization of GR, in order to incorporate the spin contributions to gravitational phenomena, is the ECT in the context of which the spacetime torsion is physically generated through the presence of spin of matter. As a matter of fact, within this model, both energy-momentum and spin angular momentum of matter act as sources of the gravitational interaction. However, since the equation governing the torsion tensor is of pure algebraic type, the torsion tensor could not propagate in the absence of spin effects, namely, outside the matter distribution and thus, in

the case of spin-less matter, gravitational equations of ECT are identical to those of GR [31]. Within the past decades, Poincaré gauge theory (PGT) of gravitation have been developed and have become a viable alternative to the GR. From physical viewpoint (and also geometrically) it is reasonable to consider gravity as a gauge theory of the local Poincaré symmetry of Minkowski spacetime. A formulation of gravity based on local gauge symmetry of spacetime geometry, i.e., the quadratic PGT, has been presented in [30, 32, 33, 34, 35, 36, 37]. In this theory, the gravitational field is described via interacting metric and torsion fields and is generated by means of EMT and spin momentum tensor of gravitating matter. The dynamical feature of spacetime torsion is decided by the order of the field strength tensors included within the Lagrangian; while the full linear case (ECT) bears a non-propagating torsion field, higher order correction terms describe a Lagrangian with dynamical torsion [34, 35, 38].

Since the advent of PGT, isotropic cosmological models have been constructed and studied with the aim of resolving fundamental cosmological problems [39]. It is shown that, gravitational interaction in the framework of homogeneous isotropic models, by imposing certain restrictions on model parameters, is altered in comparison with GR and can be repulsive under certain conditions, allowing thus to prevent initial singularity of the Universe as well as explaining the current accelerated expansion of the Universe without resorting to the notion of dark energy. Static spherically symmetric electro-vacuum solutions in PGT have been reported in [40] where it is shown that the spacetime torsion is induced by both the mass and the charge of the source. Black hole solutions with dynamical massless torsion in PGT have been reported in [41]. The obtained solutions are of Reissner-Nordstrom type with a Coulomb-like curvature provided by the torsion field, see also [35] and references therein. In the present work, motivated by the above considerations, we are interested in finding static spherically symmetric solutions representing wormhole geometries with zero tidal force in PGT. We then begin, in section 2, with introducing the field equations of PGT. We proceed to obtain exact wormhole solutions, with zero tidal force, satisfying WEC and NEC in section 3, for an spine-less anisotropic matter distribution. In Section 4 we discuss observational features of the obtained solutions and finally we conclude our paper and point out future works in section 5.

2 Field equations for spin-0⁺ mode

In the present section we give a brief review on PGT using the procedure already done within this area [30, 36, 37, 42, 43, 44, 45, 46, 47]. The PGT is founded on a spacetime with a Riemann-Cartan geometry, i.e., a Lorentz signature metric with a metric compatible connection. According to the ten independent parameters of the Poincaré group, we have ten gauge potentials. The gravitational field is then described by means of two sets of local gauge potentials, the four gauge potentials of the translation group i.e., the tetrad field e_i^μ and the metric compatible connection $\Gamma_{i\mu}^\nu$ which is associated with the six gauge potentials of the Lorentz group. The corresponding field strengths are the spacetime torsion

$$Q_{ij}^\mu = 2 (\partial_{[i} e_{j]}^\mu + \Gamma_{[i|\nu}^\mu e_{j]}^\nu), \quad (1)$$

for the tetrads and the spacetime curvature

$$R_{ij\mu}^\nu = 2 (\partial_{[i} \Gamma_{j]\mu}^\nu + \Gamma_{[i|\sigma}^\nu \Gamma_{j]\mu}^\sigma), \quad (2)$$

for the connection. These quantities obey the Bianchi identities

$$\nabla_{[i} Q_{jk]}^\mu \equiv R_{[ijk]}^\mu, \quad \nabla_{[i} R_{jk]}^{\mu\nu} \equiv 0, \quad (3)$$

where ∇_i is the covariant derivative associated to the connection $\Gamma_{i\mu}^\nu$. The Greek indices denote local Lorentz indices and the Latin ones are coordinate indices. The tetrads satisfy the following equalities

$$e_\mu^i e_i^\nu = \delta_\mu^\nu, \quad e_\mu^i e_j^\mu = \delta_j^i, \quad g_{ij} = e_i^\mu e_j^\nu \eta_{\mu\nu}. \quad (4)$$

The conventional action which is invariant under the Poincarè gauge group can be put into the form

$$A = \int d^4x e (\mathcal{L}_G + \mathcal{L}_M), \quad (5)$$

where $\mathcal{L}_M = \mathcal{L}_M(e, \Gamma, \Psi, \partial\Psi)$ stands for the minimally coupled Lagrangian density of matter fields (Ψ) which determines the energy momentum and spin source currents, $\mathcal{L}_G = \mathcal{L}_G(e_i^\mu, \partial_j e_i^\mu, \Gamma_{i\mu}^\nu, \partial_j \Gamma_{i\mu}^\nu) = \mathcal{L}_G(e_i^\mu, Q_{ij}^\mu, R_{ij}^{\mu\nu})$ being the gravitational Lagrangian density and $e = \det(e_i^\mu)$. As demonstrated within the aforementioned works, the field equations can be derived from the action (5) by performing independent variations with respect to the gauge potentials. These equations can then be written as the following form

$$\nabla_j H_\mu^{ij} - E_\mu^i = T_\mu^i, \quad (6)$$

$$\nabla_j P_{\mu\nu}^{ij} - U_{\mu\nu}^i = S_{\mu\nu}^i, \quad (7)$$

with the field momenta

$$H_\mu^{ij} := \frac{\partial e \mathcal{L}_G}{\partial \partial_j e_i^\mu} = 2 \frac{\partial e \mathcal{L}_G}{\partial Q_{ji}^\mu}, \quad (8)$$

$$P_{\mu\nu}^{ij} := \frac{\partial e \mathcal{L}_G}{\partial \partial_j \Gamma_i^{\mu\nu}} = 2 \frac{\partial e \mathcal{L}_G}{\partial R_{ji}^{\mu\nu}}, \quad (9)$$

and

$$E_\mu^i := e_\mu^i e \mathcal{L}_G - Q_{\mu j}^\nu H_\nu^{ji} - R_{\mu j}^{\nu\sigma} P_{\nu\sigma}^{ji}, \quad U_{\mu\nu}^i := H_{[\nu\mu]}^i. \quad (10)$$

Variation of the matter Lagrangian leaves us with the following expressions for the source terms

$$T_\mu^i = \frac{\partial e \mathcal{L}_m}{\partial e_i^\mu}, \quad S_{\mu\nu}^i = \frac{\partial e \mathcal{L}_m}{\partial \Gamma_i^{\mu\nu}}, \quad (11)$$

which are known, respectively as the Noether energy-momentum and spin density currents. As a consequence of minimal coupling principle, these two tensors satisfy suitable energy-momentum and angular momentum conservation laws [33]. As usual, the Lagrangian is assumed to be, at most, quadratic in the field strengths. Therefore, the field momenta can be expressed by linear combinations of the field strengths as

$$H_\mu^{ij} = \frac{e}{\ell^2} \sum_{n=1}^3 a_n Q_{\mu}^{(n)ji}, \quad (12)$$

$$P_{\mu\nu}^{ij} = -\frac{a_0 e}{\ell^2} e_{[\mu}^i e_{\nu]}^j + \frac{e}{\kappa} \sum_{n=1}^6 b_n R_{\mu\nu}^{(n)ji}, \quad (13)$$

where the three $Q_{\mu}^{(n)ji}$ and the six $R_{\mu\nu}^{(n)ji}$ are the algebraically irreducible parts of the torsion and curvature tensors, respectively; ℓ and κ are coupling constants and a_n, b_n are free coupling parameters. The torsion tensor is decomposed into its three irreducible components known as the vector, axial and tensor part as

$$Q_i = Q_{ij}^j, \quad Z_i = \frac{1}{2} \epsilon_{ijkm} Q^{jkm}, \quad D_{ijk} = Q_{i(jk)} - \frac{1}{3} Q_i g_{jk} + \frac{1}{3} g_{i(j} Q_{k)}, \quad (14)$$

whence the torsion tensor can be re-expressed as

$$Q_{ijk} = \frac{4}{3} D_{[ij]k} + \frac{2}{3} Q_{[i} g_{j]k} + \frac{1}{3} \epsilon_{ijkm} Z^m. \quad (15)$$

In PGT, in addition to the dynamical nature of spacetime metric (described by the translational gauge potential) the rotational gauge potential assumes some independent dynamics. The various dynamic modes in PGT, beyond those of metric, were first studied through the linearized theory [44, 48]. The dynamics of connection, which can be described by the torsion tensor, is represented in terms of six modes with certain spins and parity as, 2^\pm , 1^\pm and 0^\pm . A reasonable dynamic mode should transport positive energy and should not propagate outside the forward null cone, criterion often referred to as absence of ghost and tachyon. Investigations of the linearized quadratic PGT revealed that at most three modes can be simultaneously dynamic. The results of Hamiltonian analysis also found to be consistent with those of linearized investigation [37, 49]. A careful scrutiny of the Hamiltonian and propagation [50, 51, 52, 53] led to conclusion that the effects due to nonlinearities could be expected to render all of these cases physically unacceptable, with the exception of two scalar connection modes with spin 0^+ and spin- 0^- . In this regard, a cosmological model (with flat FLRW spacetime) has been studied in [54, 55] and it was found that the 0^+ mode naturally couples to the acceleration of the Universe and could account for current observations. The extension of this model to include spin- 0^- mode has also been studied in [56], see also [57] for a beautiful generalization of torsion cosmology models. In the present study we only consider the simple spin- 0^+ case, then, we choose $a_2 = -2a_1$, $a_3 = -a_1/2$ and except for $b_6 \neq 0$, we assume all the b_n coefficients to vanish, see also [50] for more details. The associated gravitational Lagrangian density for this mode then reads

$$\mathcal{L}_G = -\frac{a_0}{2}R + \frac{b_6}{24}R^2 + \frac{a_1}{8}[Q_{\nu\sigma\mu}Q^{\nu\sigma\mu} + 2Q_{\nu\sigma\mu}Q^{\mu\sigma\nu} - 4Q_\mu Q^\mu], \quad Q_\mu = Q_{\mu\nu}{}^\nu, \quad (16)$$

where physical reasonability on kinetic energy requires that $a_1 > 0$ and $b_6 > 0$. Moreover, the Newtonian limit requires $a_0 = -(8\pi G)^{-1} = -1$ [44], where we have set the unites so that $8\pi G = c = 1$. For a vanishing spin source ($S_{\mu\nu}{}^i = 0$) one can perform variation of gravitational Lagrangian (16) with respect to the gauge potentials. This gives, for Eq. (7), the following equations [55]

$$\nabla_\nu R = -\frac{2}{3}\left[R + \frac{6\mu}{b_6}\right]Q_\nu, \quad Z_\nu = 0, \quad D_{\mu\nu}\sigma = 0, \quad (17)$$

where $\mu = a_1 - a_0$ is the effective mass of the linearized 0^+ mode. The second and third parts of Eq. (17) leave us with the following constraint on torsion tensor

$$Q_{ij}{}^\mu = \frac{2}{3}Q_{[i}e_{j]}{}^\mu, \quad (18)$$

with the help of which, Eq. (6) can be rewritten as [55]

$$\nabla_j H_\mu{}^{ij} - E_\mu{}^i = e\left\{\frac{2a_1}{3}\left[e_\nu^i \nabla_\mu Q^\nu - e_\mu^i \tilde{\nabla}_j Q^j\right] + e_\mu^i \left[\frac{a_0}{2}R - \frac{b_6}{24}R^2 + \frac{a_1}{3}Q_i Q^i\right] + R_\mu{}^i \left(\frac{b_6}{6}R - a_0\right)\right\} = T_\mu{}^i. \quad (19)$$

Next, in order to better deal with Eq. (19) and first part of (17), one can rewrite them in terms of metric g_{jk} and torsion $Q_{ij}{}^k$. By doing so, one arrives at the following field equations [55]

$$a_0 \tilde{G}_{ij} + T_{ij} + \bar{T}_{ij} = 0, \quad (20)$$

$$\tilde{\nabla}_i R + \frac{2}{3}\left[R + \frac{6\mu}{b_6}\right]Q_i = 0, \quad (21)$$

where $\tilde{\nabla}_i$ stands for covariant derivative with respect to Levi-Civita connection $\tilde{\Gamma}_{ij}{}^k$ and \tilde{G}_{ij} is the standard Einstein tensor. The tensor \bar{T}_{ij} represents the contribution due to scalar torsion mode and is given by

$$\bar{T}_{ij} = -\frac{\mu}{3}\left[\tilde{\nabla}_i Q_j + \tilde{\nabla}_j Q_i - 2g_{ij}\tilde{\nabla}_k Q^k\right] - \frac{\mu}{9}\left[2Q_i Q_j + g_{ij}Q_k Q^k\right] - \frac{b_6}{6}R\left[R_{(ij)} - \frac{1}{4}g_{ij}R\right], \quad (22)$$

where we have following expressions for Ricci curvature tensor and Ricci scalar curvature, respectively, as

$$R_{ij} = \tilde{R}_{ij} + \frac{1}{3} \left[2\tilde{\nabla}_j Q_i + g_{ij} \tilde{\nabla}_k Q^k \right] + \frac{2}{9} \left[Q_i Q_j - g_{ij} Q_k Q^k \right], \quad (23)$$

$$R = \tilde{R} + 2\tilde{\nabla}_i Q^i - \frac{2}{3} Q_i Q^i. \quad (24)$$

3 Wormhole Solutions

Let us consider the general static and spherically symmetric line element representing a wormhole spacetime given by

$$ds^2 = -e^{2\Phi(r)} dt^2 + \left(1 - \frac{b(r)}{r} \right)^{-1} dr^2 + r^2 d\Omega^2, \quad (25)$$

where $d\Omega^2 = d\theta^2 + \sin^2 \theta d\phi^2$ is the standard line element on a unit two-sphere, $\Phi(r)$ is the redshift function and $b(r)$ is the wormhole shape function. The radial coordinate ranges from r_0 (wormhole's throat) to spatial infinity. Conditions on redshift and shape functions under which, wormholes are traversable have been discussed completely in [7]. Traversability of the wormhole requires that the spacetime be free of horizons which are defined as the surfaces with $e^{2\Phi(r)} \rightarrow 0$; therefore the redshift function must be finite everywhere. In the present work, we try to find $b(r)$, assuming there is no tidal force present, i.e., $\Phi(r) = \text{Constant}$ and we will set this constant to be zero for latter convenience. The non-vanishing components of the torsion tensor are given as [41]

$$Q_{tr}{}^r = Q_{t\theta}{}^\theta = Q_{t\phi}{}^\phi = \frac{B(r)}{3}, \quad Q_{tr}{}^t = Q_{\theta r}{}^\theta = Q_{\phi r}{}^\phi = \frac{B'(r)}{2B(r)}, \quad (26)$$

where we note that these components satisfy the constraints given in the second and third parts of Eq. (17). Let us define the time-like and space-like vector fields, respectively as $u^i = [1, 0, 0, 0]$ and $v^i = [0, \sqrt{1 - b(r)/r}, 0, 0]$, so that $u^i u_i = -1$ and $v^j v_j = 1$. The anisotropic EMT of matter source then takes the form

$$T_{ij} = [\rho(r) + p_t(r)] u_i u_j + p_t(r) g_{ij} + [p_r(r) - p_t(r)] v_i v_j, \quad (27)$$

with $\rho(r)$, $p_r(r)$, and $p_t(r)$ being the energy density, radial and tangential pressures, respectively. For spacetime metric (25), the field equation (20) reads (we set $\Phi(r) = 0$)

$$\begin{aligned}\rho(r) &= \frac{b_6(r-b)^2 B'^2}{8r^2 B^2} - \left\{ \frac{b_6(r-b)^2 B'^2}{4r^2 B^3} + \frac{b_6(r-b)(rb' - 4r + 3b)B'}{8r^3 B^2} \right. \\ &+ \left. \frac{(r-b)(3b_6 b' + r^2(b_6 B^2 + 9\mu))}{9r^3 B} \right\} B'' + \frac{3b_6(r-b)^2 B'^4}{32r^2 B^4} + \frac{b_6(r-b)(rb' - 4r + 3b)B'^3}{8r^3 B^3} \\ &+ \left\{ b_6(r-b)r^3 B^2 + 27b_6 b^2 - 72(\mu r^2 + b_6)rb + 24(3\mu r^2 + 2b_6)r^2 - 6b_6 r b b' + 3b_6 r^2 b'^2 \right\} \frac{B'^2}{96r^4 B^2} \\ &+ \frac{9b_6 b'^2 - 6r^2(9a_0 - b_6 B^2)b' + r^4 B^2(b_6 B^2 + 18\mu)}{54r^4} \\ &+ \frac{[3b_6 b' + r^2(b_6 B^2 + 9\mu)](rb' - 4r + 3b)}{18r^4 B} B',\end{aligned}\tag{28}$$

$$\begin{aligned}p_r(r) &= \frac{3b_6(r-b)^2 B'^2}{8r^2 B^2} + \frac{9b_6(r-b)^2 B'^4}{32r^2 B^4} + \frac{b_6(r-b)[3rb' - 8r + 5b]B'^3}{8r^3 B^3} - \left\{ \frac{3b_6(r-b)^2 B'^2}{4r^2 B^3} \right. \\ &- \left. \frac{b_6(r-b)[3rb' - 4r + b]B'}{8r^3 B^2} + \frac{b_6(r-b)[rb' - b + \frac{2}{9}r^3 B^2]}{2r^4 B} \right\} B'' \\ &+ \left\{ 27b_6 r^2 b'^2 + 18b_6 r(4r - 7b)b' + 40b_6 r^3(r-b)B^2 - 117b_6 b^2 \right. \\ &- \left. 216r \left[\mu r^2 - \frac{4}{3}b_6 \right] b + 216r^2 \left[\mu r^2 - \frac{2}{3}b_6 \right] \right\} \frac{B'^2}{288r^4 B^2} \\ &+ \left\{ 9b_6 r^2 b'^2 + 2b_6 r[r^3 B^2 - 6r - 3b]b' - 2b_6 r^3 b B^2 \right. \\ &- \left. 27b_6 b^2 + (18b_6 r - 36\mu r^3)b + 36\mu r^4 \right\} \frac{B'}{36r^5 B} \\ &+ \frac{27b_6 r b'^2 + 12b_6[r^3 B^2 - \frac{9}{2}b]b' + [b_6 r^3 B^4 - 18(\mu r^3 + b_6 b)B^2 + 162a_0 b]r^2}{162r^5},\end{aligned}\tag{29}$$

$$\begin{aligned}p_t(r) &= -\frac{b_6(r-b)^2 B'^2}{8r^2 B^2} - \frac{3b_6(r-b)^2 B'^4}{32r^2 B^4} - \frac{b_6(r-b)[rb' - 2r + b]B'^3}{8r^3 B^3} + \left\{ \frac{b_6(r-b)^2 B'^2}{4r^2 B^3} \right. \\ &+ \left. \frac{b_6(r-b)(rb' - b)B'}{8r^3 B^2} + \frac{(r-b)[12\mu r^3 + b_6 r b' - 3b_6 b]}{12r^4 B} \right\} B'' \\ &- \left\{ b_6 r^2 b'^2 + b_6(4r - 6b)rb' + \frac{8}{9}b_6 r^3(r-b)B^2 - 11b_6 b^2 \right. \\ &- \left. 4(6\mu r^2 - 7b_6)rb + 8(3\mu r^2 - 2b_6)r^2 \right\} \frac{B'^2}{32r^4 B^2} \\ &- \left\{ b_6 r^2 b'^2 + [(12\mu r^2 + 4b_6)r^2 - 8b_6 r b]b' \right. \\ &+ \left. \frac{8b_6}{3}r^3(r-b)B^2 - 9b_6 b^2 + 12(\mu r^2 + b_6)rb - 24\mu r^4 \right\} \frac{B'}{24r^5 B} \\ &+ \frac{[3b_6 r^3 B^2 + 81a_0 r^3 + 27b_6 b]b' + [b_6 r^3 B^4 + 9(b_6 b - 2\mu r^3)B^2 - 81a_0 b]r^2}{162r^5}.\end{aligned}\tag{30}$$

For the temporal and radial components of the field equation (21) we have, respectively

$$\begin{aligned}
& \left[1 - \frac{b}{r}\right] (B'^2 - 2BB'') + \left[\frac{b'}{r} - \frac{4}{r} + \frac{3b}{r^2}\right] BB' + \frac{4}{9} \left[\frac{3b'}{r^2} + B^2 + \frac{9\mu}{b_6}\right] B^2 = 0, \quad (31) \\
& \left[9 \left(1 - \frac{b}{r}\right) \frac{B'}{B^2} + \frac{9rb' - 12r + 3b}{2r^2 B}\right] B'' - \frac{9(r-b)B'^3}{2rB^3} - \frac{9rb' - 24r + 15b}{2r^2 B^2} B'^2 \\
& + \left\{9b_6 r^2 b'' + [4b_6 r^3 B^2 - 36\mu r^3 + 6b_6 r b' + 36b_6 r - 54b_6 b]\right\} \frac{B'}{6b_6 r^3 B} \\
& - \frac{3r^2(r-b)B''' - 2rBb'' + 4b'B}{r^3 B} = 0 \quad (32)
\end{aligned}$$

where a prime denotes d/dr . The above two equations can be solved simultaneously for the shape function with a general solution given by

$$b(r) = \left\{C_1 - \frac{1}{3} \int r F_1(r) e^{3 \int F_2(r) dr} dr\right\} e^{-3 \int F_2(r) dr}, \quad (33)$$

where

$$\begin{aligned}
F_1(r) &= \frac{4rB^3 + \frac{36\mu r}{b_6} B - 18rB'' + 9r\frac{B'^2}{B} - 36B'}{3rB' + 4B}, \\
F_2(r) &= \frac{2rBB'' - rB'^2 + 3BB'}{B(3rB' + 4B)}, \quad (34)
\end{aligned}$$

and C_1 is an integration constant. Now, assuming a power-law behavior for torsion, $B(r) = B_0 r^n$ ($n < 0$ and $n \neq -4/3, -2$), the integration can be performed giving

$$b(r) = \alpha_1 r + \alpha_2 r^3 + \alpha_3 r^{2n+3} + \alpha_4 r^{-\frac{3n(n+1)}{3n+4}}, \quad (35)$$

where

$$\begin{aligned}
\alpha_1 &= \frac{3n(n+2)}{3n^2 + 6n + 4}, \quad \alpha_2 = -\frac{4\mu}{b_6(n+2)^2}, \quad \alpha_3 = -\frac{4B_0^2}{3(9n^2 + 20n + 12)}, \quad (36) \\
\alpha_4 &= -\alpha_3 r_0^{\frac{9n^2+20n+12}{3n+4}} - \alpha_2 r_0^{\frac{3(n+2)^2}{3n+4}} + \frac{4\alpha_1}{3n(n+2)} r_0^{\frac{3n^2+6n+4}{3n+4}}, \quad (37)
\end{aligned}$$

and use has been made of the condition $b(r_0) = r_0$ with r_0 being the wormhole throat. The shape function has to satisfy the flare-out condition $rb' - b < 0$ which leads to the following inequality at the throat

$$-\frac{4r_0 (b_6 (B_0^2 r_0^{2n+2} + 3) + 9\mu r_0^2)}{3b_6(3n+4)} < 0. \quad (38)$$

Next we proceed to obtain the energy density, radial and tangential pressures for our solution. These quantities take the form

$$\rho(r) = \beta_1 - (2n+3)(a_0 + \mu)\alpha_3 r^{2n} - (a_0 + \mu)\alpha_1 r^{-2} + \frac{3n(n+1)(a_0 + \mu)}{3n+4} \alpha_4 r^{-\frac{3(n+2)^2}{3n+4}} \quad (39)$$

$$p_r(r) = \gamma_1 + (a_0 + \mu)\alpha_3 r^{2n} + (a_0 + \mu)\alpha_1 r^{-2} + (a_0 + \mu)\alpha_4 r^{-\frac{3(n+2)^2}{3n+4}}, \quad (40)$$

$$p_t(r) = \gamma_1 + (n+1)(a_0 + \mu)\alpha_3 r^{2n} - \frac{(a_0 + \mu)(3n^2 + 6n + 4)}{2(3n + 4)}\alpha_4 r^{\frac{-3(n+2)^2}{3n+4}}, \quad (41)$$

where

$$\beta_1 = \frac{3\mu(8a_0 - \mu(n^2 + 4n - 4))}{2b_6(n+2)^2}, \quad (42)$$

$$\gamma_1 = \frac{\mu(-8a_0 + \mu(3n^2 + 12n + 4))}{2b_6(n+2)^2}. \quad (43)$$

In the framework of classical GR, the fundamental flaring-out condition results in the violation of NEC. Such a violation can be surveyed by applying the focusing theorem on a congruence of null rays, defined by a null vector field k^μ , where $k^\mu k_\mu = 0$ [9, 58]. For the EMT given in (27) the NEC is given by

$$\rho(r) + p_r(r) \geq 0, \quad \rho(r) + p_t(r) \geq 0. \quad (44)$$

For the sake of physical reliability of the solutions, we require that the wormhole configuration respects the WEC given by the following inequalities

$$\rho(r) \geq 0, \quad \rho(r) + p_r(r) \geq 0, \quad \rho(r) + p_t(r) \geq 0. \quad (45)$$

Using expressions (39)-(41) we then get

$$\rho(r) + p_r(r) = \beta_1 + \gamma_1 - 2(n+1)(a_0 + \mu)\alpha_3 r^{2n} + \frac{3n^2 + 6n + 4}{3n + 4}(a_0 + \mu)\alpha_4 r^{\frac{-3(n+2)^2}{3n+4}}, \quad (46)$$

$$\rho(r) + p_t(r) = \beta_1 + \gamma_1 - (n+2)(a_0 + \mu)\alpha_3 r^{2n} - (a_0 + \mu)\alpha_1 r^{-2} + \frac{(a_0 + \mu)(3n^2 - 4)}{2(3n + 4)}\alpha_4 r^{\frac{-3(n+2)^2}{3n+4}}. \quad (47)$$

Thus, the energy conditions at the throat take the form

$$\rho(r)\Big|_{r=r_0} = \frac{8B_0^2 b_6 (a_0 + \mu) r_0^{2n+2} + 9[-2a_0 b_6 n + 8a_0 \mu r_0^2 - 2b_6 \mu n + \mu^2(4 - 3n)r_0^2]}{6b_6(3n+4)r_0^2} \geq 0, \quad (48)$$

$$\rho(r) + p_r(r)\Big|_{r=r_0} = \frac{4(a_0 + \mu)[b_6(B_0^2 r_0^{2n+2} + 3) + 9\mu r_0^2]}{3b_6(3n+4)r_0^2} \geq 0, \quad (49)$$

$$\rho(r) + p_t(r)\Big|_{r=r_0} = \frac{(a_0 + \mu)[b_6(2B_0^2 r_0^{2n+2} - 9n - 6) + 18\mu r_0^2]}{3b_6(3n+4)r_0^2} \geq 0. \quad (50)$$

The set of parameters $\mathbf{M} = \{n, b_6, \mu, B_0, a_1\}$ construct a 5-dimensional parameter space that the allowed regions of which are determined through physically reasonable conditions on wormhole configuration. We therefore require that the shape function satisfies the flare-out condition at the throat, i.e., the inequality (38). The supporting matter for wormhole configuration must obey the WEC, i.e., inequalities given in (45). We note that WEC implies the null form. In order that the energy conditions be satisfied at the throat the inequalities (48)-(50) must be fulfilled. Moreover, the coefficients of r within the expressions (39), (46) and (47) must be positive so that the energy conditions hold throughout the spacetime. We also demand $n < 0$ so that the torsion converges asymptotically. Hence, as $r \rightarrow \infty$, the coefficient of α_4 within the solution (35) vanishes for $-4/3 < n < -1$. For the coefficient of α_3 to get vanished at large values of coordinate radius, we must have $n < -3/2$. This is not allowed for n parameter regarding the shaded region of Fig. (1). However, as $r \rightarrow \infty$ if we neglect the effects of the coefficient of α_3 in comparison with that of α_2 , the solution may be asymptotically de-Sitter (anti

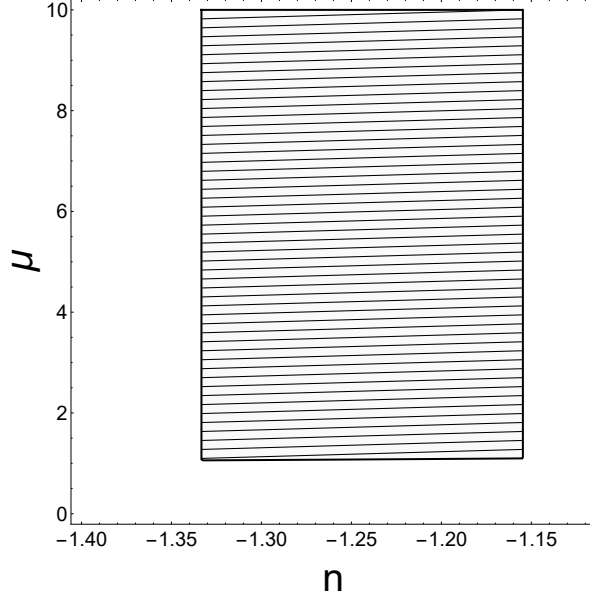


Figure 1: The allowed values of μ and n parameters (shaded region) for $B_0 = 0.001$, $b_6 = 100$, $r_0 = 1$ and $a_0 = -1$.

de-Sitter) depending on the signs of μ and b_6 parameters. In Hamiltonian analysis of scalar modes of PGT [50], the positivity of kinetic energy requires that $b_6 > 0$ and $a_1 > 0$. The last condition also leads to $\mu > 0$. Thus, the wormhole spacetime asymptotes an anti de-Sitter spacetime with cosmological constant $\Lambda = -12\mu/[b_6(n+2)^2] < 0$. The solution is however asymptotically de-Sitter if one relaxes the condition on positivity of kinetic energy allowing thus for $\mu < 0$. This case could mimic the cosmological constant and other cosmological scenarios with negative kinetic energy [59]. Figure (1) presents a 2D subspace of the 5D parameter space constructed out of the allowed values of μ and n parameters. For any point within the shaded region of this subset of \mathbf{M} the above mentioned conditions are respected. The Left panel of Fig. (2) presents the inverse of the radial metric component (g_{rr}^{-1}). We observe that g_{rr}^{-1} is positive for $r > r_0$ and thus the metric signature is preserved for radii bigger than the throat radius. As the right panel shows, the energy density and the quantities $\rho + p_r$ and $\rho + p_t$ remain positive for the allowed values of Fig. (1); thus the WEC is satisfied throughout the spacetime. Following the results of [7], one finds that the wormhole configuration needs exotic matter, i.e, a kind of matter that does not obey WEC and NEC. Therefore, one may define a measure of exoticity of matter through the exoticity parameter ξ , given as [7],[58]

$$\xi(r) = \frac{\tau(r) - \rho(r)}{|\rho(r)|} = -\frac{\rho(r) + p_r(r)}{|\rho(r)|}, \quad (51)$$

where, $\tau(r) = -p_r(r)$ is the radial tension. The positiveness of $\xi(r)$ signals exotic behavior of the matter. Fig. (3) shows the behavior of exoticity parameter for allowed values of model parameters. It is seen that this parameter is negative at the throat and stays negative for $r > r_0$. Thus, there is no need of introducing exotic matter in order to construct the present wormhole solutions.

The wormhole configurations we have presented so far respect NEC and WEC with a non-exotic fluid as the supporting matter. In order to get a better understanding of the behavior of such a type of matter we proceed with considering a linear relation between pressure profiles and energy density

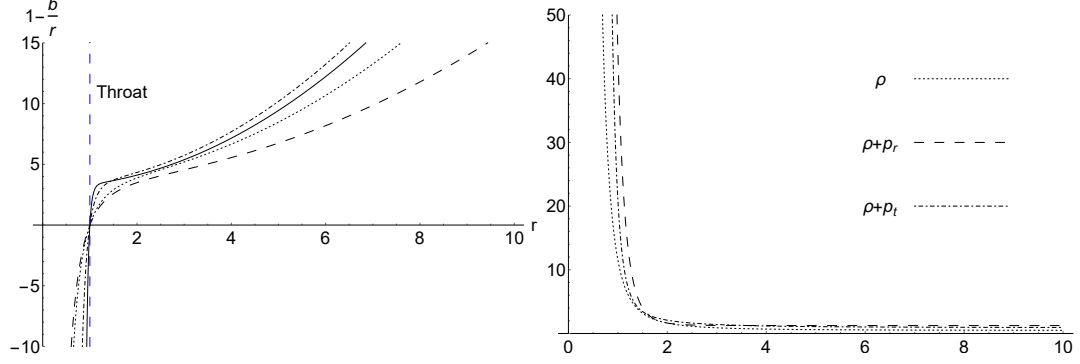


Figure 2: Left panel: behavior of inverse of radial metric component for $n = -1.21, \mu = 3.1$ (dotted curve), $n = -1.19, \mu = 2.1$ (dashed curve), $n = -1.28, \mu = 3.6$ (dot-dashed curve) and $n = -1.312, \mu = 3.0$ (solid curve). Right panel: Behavior of $\rho(r)$ for $n = -1.19$ and $\mu = 2.3$, $\rho + p_r$ for $n = -1.25$ and $\mu = 3.5$ and $\rho + p_t$ for $n = -1.27$ and $\mu = 3.0$. We have also set $B_0 = 0.001$, $b_6 = 100$, $r_0 = 1$ and $a_0 = -1$. The blue dashed line indicates the location of the throat.

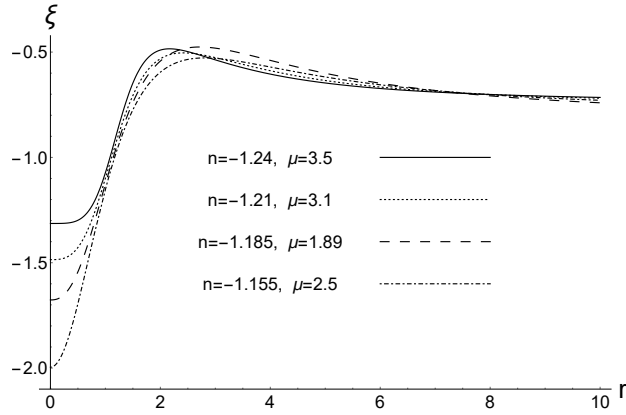


Figure 3: Plot of exoticity against radial coordinate for $B_0 = 0.0010$, $b_6 = 100$, $r_0 = 1$ and $a_0 = -1$.

with r-dependent state parameters as

$$p_r(r) = w_r(r)\rho(r), \quad p_t(r) = w_t(r)\rho(r). \quad (52)$$

The state parameters will take the following form at the throat

$$w_{r0} = w_r(r_0) = \frac{3(3n+4)[2a_0b_6 + \mu(2b_6 + 3\mu r_0^2)]}{8B_0^2b_6(a_0 + \mu)r_0^{2n+2} - 9[2a_0(b_6n - 4\mu r_0^2) + \mu(2b_6n + \mu(3n-4)r_0^2)]}, \quad (53)$$

$$w_{t0} = w_t(r_0) = \frac{-4B_0^2b_6(a_0 + \mu)r_0^{2n+2} - 3[4a_0(b_6 + 3\mu r_0^2) + \mu(4b_6 - 9\mu n r_0^2)]}{8B_0^2b_6(a_0 + \mu)r_0^{2n+2} + 9(-2a_0b_6n + 8a_0\mu r_0^2 - 2b_6\mu n + \mu^2(4-3n)r_0^2)}. \quad (54)$$

At first glance, depending on the model parameters, the radial and tangential state parameters at wormhole throat can assume different values. However these values are subject to physical conditions stated before. Let us begin by solving the above two expressions for n and μ parameters in terms of the rest ones. The solutions read

$$n_{1,2} = \frac{1}{27b_6(1+w_{r0})(w_{r0}-2w_{t0}-1)} \left\{ 9X(\pm 2w_{t0} \mp w_{r0} \pm 1) + 18b_6(w_{r0}^2 - 4w_{t0}(1+w_{t0}) - 1) \right\} \\ + \frac{2[B_0^2 + 9 + w_{r0}(3-B_0^2) + 2w_{t0}(3+B_0^2)]}{-9(1+w_{r0})}, \quad (55)$$

$$\mu_{1,2} = \frac{-b_6(1+w_{r0}+2w_{t0}) \pm X}{3(1-w_{r0}+2w_{t0})}, \quad (56)$$

where

$$X = 2 \left[b_6(1+w_{r0}+2w_{t0})(b_6(1+w_{r0}+2w_{t0}) - 6a_0(1-w_{r0}+2w_{t0})) \right]^{\frac{1}{2}}, \quad (57)$$

and we have set $r_0 = 1$ for later convenience. With the help of these solutions we are able to obtain possible bounds on state parameters at the throat regarding the physical reasonability conditions. Considering the allowed region as provided in Fig (1), we require that

$$-1.33 < n_{1,2} \leq -1.154, \quad 1 \leq \mu_{1,2} < \infty. \quad (58)$$

The above inequalities put restrictions on the state parameters w_{r0} and w_{t0} that the allowed values of which has been plotted in the Left panel of Fig. (4). It is then observed that the lower bounds on the state parameters are $-0.033 \lesssim w_{r0}$ and $-0.56 \lesssim w_{t0}$ so that both WEC and NEC are fulfilled at the throat. As discussed in [55], there is not too much constraint on the μ parameter, except for its positivity and finiteness as a mass parameter, since the baryonic matter will only interact with the scalar torsion mode indirectly by gravitation. In the right panel, we have plotted for state parameters versus radial coordinate. These parameters assume different values depending on the model parameters. As long as $r_0 < r < r_1$, where r_1 is the radial coordinate at which $w_r(r_1) = 0$, the radial pressure is positive; however, we have a dust-like behavior in radial direction at $r = r_1$. For $r_1 < r < \infty$ the radial pressure becomes negative and asymptotically tends to the dashed red line which is the equation of state of a string gas, $p = -1/3\rho$. The state parameter in tangential direction remains always negative and asymptotically reaches the same equation of state as its counterpart in radial direction. We can therefore observe that the wormhole configuration is isotropic at $r \rightarrow \infty$. This behavior can be further investigated through the anisotropic parameter, defined as, $\Delta(r) = p_t(r) - p_r(r) = [w_t(r) - w_r(r)]\rho(r)$. Since $\rho(r) > 0$ throughout the spacetime, it is the sign of the term in square brackets that decide the geometry of wormhole configuration. Let us define the coordinate radius r_2 so that for $r_0 < r_2 < \infty$ we have $\Delta(r_2) = 0$, see the left panel of Fig. (5). We therefore note that since the ratio $2\Delta/r$ represents the force due to anisotropic nature of the configuration, we have an attractive geometry for $r_0 < r < r_2$ and a repulsive geometry for $r_2 < r < \infty$. The value of coordinate radius r_2 depends on model

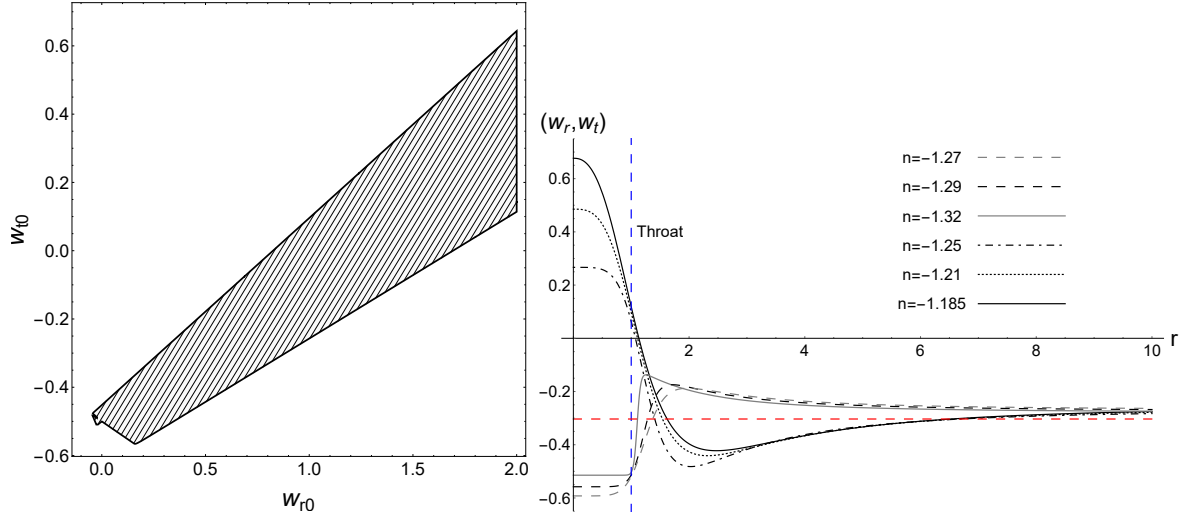


Figure 4: Left panel: The allowed values (shaded region) of state parameters at the wormhole throat. Right panel: The behavior of state parameters w_r (solid, dotted and dot-dashed curves) and w_t (dashed, gray, and gray dashed) for different values of n parameter. We have set $B_0 = 0.001$, $b_6 = 100$, $a_0 = -1$ and $\mu = 5$ (for the right panel). The dashed red line represents the asymptotic behavior of the state parameters and corresponds to equation of state of cosmic strings. The blue dashed line indicates the location of the throat.

parameters, specifically for the present case, the smaller the absolute value of n parameter, the larger the value of coordinate radius r_2 . Moreover, having passed the negative values ($r > r_2$), the anisotropy parameter reaches a maximum, say $r_3 > r_2$, at which $\Delta'(r_3) = 0$. As the left panel shows, the larger the absolute value of n parameter, the closer the maximum value of anisotropy to the throat. One then may intuitively imagine that the rate of growth of spacetime torsion around the throat could affect the anisotropy of the wormhole configuration. As $r \rightarrow \infty$ we have $\Delta(r) \rightarrow 0$, thus asymptotically, the supporting matter of the wormhole configuration tends to an isotropic fluid.

4 Observational Features

One of the interesting ways for detecting wormholes is to search for their gravitational lensing effects. In the present section we investigate lensing features of the obtained wormhole solutions. To this aim we need to study the behavior of null geodesics traveling within the wormhole spacetime. The starting point of our study is the following Lagrangian for lightlike geodesics, given by

$$2\mathcal{L} = g_{\mu\nu} \dot{x}^\mu \dot{x}^\nu = -\dot{t}^2 + \left(1 - \frac{b(r)}{r}\right)^{-1} \dot{r}^2 + r^2 \dot{\phi}^2, \quad (59)$$

where use has been made of the spacetime metric (25) and an overdot denotes derivative with respect to the curve parameter η . Because of the spherical symmetry we consider the equatorial plane $\theta = \pi/2$. The Lagrangian $\mathcal{L}(\dot{x}, x)$ is constant along a geodesic curve, so one can classify the spacetime geodesics as, timelike geodesics (the world lines of freely falling particles) for which $\mathcal{L} < 0$, lightlike ones (light rays) for which $\mathcal{L} = 0$ and spacelike geodesics for which $\mathcal{L} > 0$. Equation of photon trajectory then takes form

$$\dot{r}^2 + \left(1 - \frac{b(r)}{r}\right) \left(\frac{h^2}{r^2} - \mathcal{E}^2\right) = 0, \quad (60)$$

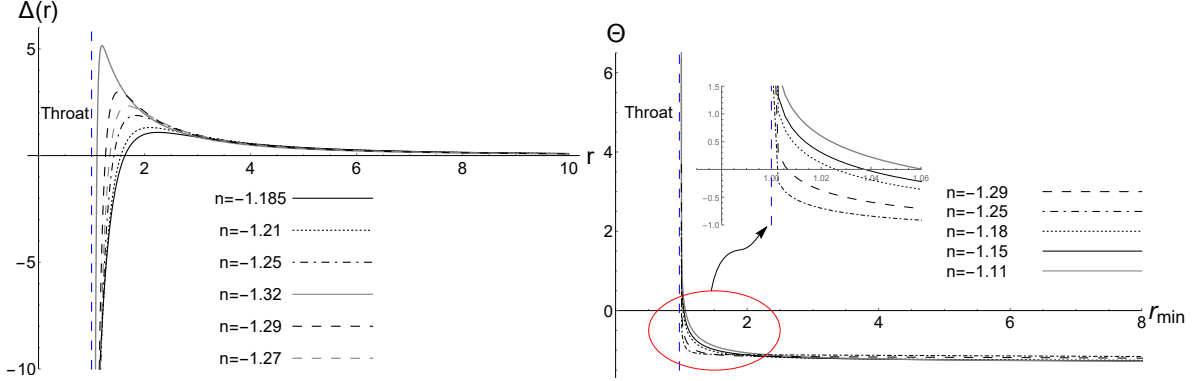


Figure 5: Left panel: The behavior of anisotropy parameter against the radial coordinate for different values of parameter n and $B_0 = 0.001$, $b_6 = 100$, $\mu = 5$, $r_0 = 1$ and $a_0 = -1$. Right panel: Deflection angle against closest distance approach for different values of n parameter. We have also set $B_0 = 0.001$, $b_6 = 100$, $r_0 = 1$, $\mu = 1.83$ and $a_0 = -1$. The blue dashed line indicates the location of the throat.

where $\mathcal{E} = \dot{t}$ is the total energy of the particle moving on its orbit, $h = r^2 \dot{\phi}$ is its specific angular momentum. Consider now a light ray incoming from infinity, reaching the minimum distance r_{\min} from the center of the gravitating body, emerging then in another direction. The deflection angle of the light ray as a function of the closet distance approach is then given by [60]

$$\Theta(r_{\min}) = -\pi + 2 \int_{r_{\min}}^{\infty} \frac{\mu dr}{[(r^2 - rb(r))(r^2 - \mu^2)]^{\frac{1}{2}}}, \quad (61)$$

where $\mu = h/\mathcal{E}$ is the impact parameter and $dr/d\phi = 0$ at $r = r_{\min}$ so we have $\mu = r_{\min}$. Utilizing solution (35), we obtain the deflection angle as

$$\Theta(r_{\min}) = -\pi + 2r_{\min} \int_{r_{\min}}^{\infty} (r^2 - r_{\min}^2)^{-\frac{1}{2}} \left[r^2 - \alpha_1 r^2 - \alpha_2 r^4 - \alpha_3 r^{2(n+2)} - \alpha_4 r^{\frac{4-3n^2}{3n+4}} \right]^{-\frac{1}{2}} dr. \quad (62)$$

In the right panel of Fig. (5) we have plotted for deflection angle as a function closest distance approach using numerical methods. It is therefore seen that the more the closest distance decreases, the more the deflection angle grows. Decreasing r_{\min} further causes the light ray to infinitesimally come closer to the photon orbit making it to wind up for a large number of times before emerging out. The deflection angle will diverge, eventually, at a critical value of closet distance approach, r_{\min}^{cr} where light ray will loop around a circular photon orbit indefinitely. The set of these orbits constructs the photon sphere satisfying $\dot{r} = \ddot{r} = 0$ [61] [62]. In [63], it has been shown that the wormhole throat can act as an effective photon sphere located at $r_{\min}^{\text{cr}} = r_0$. Hence, as $r_{\min} \rightarrow r_0$, the deflection angle increases and diverges at the wormhole throat where an unstable photon sphere is present. As a result, the wormhole can produce infinite number of relativistic images of an appropriately placed light source. This infinite sequence corresponds to infinitely many light rays whose limit curve asymptotically spirals towards the unstable photon sphere [61]. Since the photon sphere coincides with the wormhole throat, such a sphere can be detected utilizing thoroughly and carefully designed modern instruments [62],[64], providing thus, possible observational proofs for the existence of the wormhole. The deflection angle decreases as r_{\min} increases beyond r_0 (the light bears lesser bending) until the closest distance approach reaches a critical value at which $\Theta(r_{\min}^*) = 0$, i.e., no deflection of light occurs at all, see the inset of Fig. (5). In such a situation, any incoming light ray from infinity that reaches the coordinate distance $r = r_{\min}^*$, is scattered back to infinity without any spinning around the wormhole lens. Therefore the

light ray does not undergo any net deflection by the gravitating object. For $r_{\min} > r_{\min}^*$ the deflection angle is found to be negative, which can be interpreted as there is a repulsion of light by the wormhole configuration. A negative value for deflection angle has also been reported in gravitational lensing by a naked singularity [65].

The phenomenon of gravitational lensing is nowadays a powerful tool for probing in astrophysics and cosmology in order to address open problems such as, *i*) spatial distribution of mass at large distances, *ii*) the interaction of baryons and dark matter and its effects of the shape of galaxies, *iii*) the overall geometry, content and kinematics of the Universe and *iv*) investigating distant galaxies, black holes, and active nuclei that are too small or too dim to be detected with current observational tools [66]. However, beside the lensing effects that can play a major role in detecting wormhole configurations, various observational aspects have been perused so far with the aim of probing wormholes living in our Universe, among which we can quote: the study of particle trajectory in the wormhole spacetime [67], accretion disks around wormholes [68] and their gravitational wave signatures [69]. Another interesting candidate for extracting physical information from the wormhole spacetime is the shadow cast by it or its apparent shape [70]. As the shape of the shadow is merely determined by the background metric, the observation of such a phenomenon can provide useful information on the nature of the compact object and under some conditions this interesting event can provide observational testbed for distinguishing the wormhole from other compact bodies. This idea has motivated many researchers to investigate different aspects of wormhole shadows. Work along this line has been carried out, e.g., shadows cast by rotating [71] and charged wormholes [72] has been studied and in [73] the authors have developed the shadow-like images of wormholes surrounded by optically thin dust. The existence of unstable photon orbits is of crucial importance in studying wormhole shadows as these orbits define the boundary between capture and non-capture of the light rays around a wormhole configuration. Thus, the boundary of the shadow is only determined by the metric of spacetime since it corresponds to the apparent shape of the photon sphere as seen by a distant observer [71, 74] (see also [75] for more details). As the lensing effects and shadows are of significant importance for detecting astrophysical compact objects, especially wormholes, it is about time to probe the existence of such objects utilizing advanced instruments, e.g., the US-led Event Horizon Telescope (EHT) project³ and the European Black Hole Cam (BHC) project⁴.

5 Concluding Remarks

Static spherically symmetric configurations representing wormhole geometries with zero tidal force, were studied for a subclass of PGT Lagrangians that allow for spin-0⁺ propagating modes. In contrast to ECT where spacetime torsion has a non-dynamic nature driven by spin of fermionic particles, the PGT allows for dynamic torsion in addition to spacetime curvature, even if the spin effects are absent. By specifying the non-vanishing components of the torsion tensor, we obtained the field equations for an anisotropic spin-less matter distribution. The field equation derived from variation of gravitational Lagrangian with respect to the connection results in two coupled differential equations for the shape function, $b(r)$ and torsion component, $B(r)$. The solution came up as an integral relating the behavior of the shape function to the spacetime torsion. Assuming then a power-law behavior for torsion component, $B(r) = B_0 r^n$, the shape function was obtained in terms of model parameters. We then provided the allowed region for two of the model parameters (n and μ) for which the conditions on physical reasonability of the model are respected. For the obtained solutions, the matter supporting the wormhole geometry obeys the WEC and NEC. We also assumed that the radial and tangential profiles of the fluid pressure depend linearly on energy density via different r -dependent state parameters. The behavior of the state parameters was investigated and it was found that the matter threading the wormhole throat can assume different equations of state (at the throat) depending on the model

³Project website: www.eventhorizontelescope.org

⁴Project website: www.blackholecam.org

parameters, especially in the present work, the rate of growth of torsion as decided by the exponent n . Furthermore, we provided the allowed values of state parameters at the throat subject to fulfillment of conditions on physical validity of the solutions. The anisotropy parameter for wormhole geometry was studied and it was observed that this parameter could admit different maxima near the throat depending on the growth rate of spacetime torsion. Finally we investigated gravitational lensing effects on the wormhole's surrounding environment and it was found that the deflection angle of the incoming beam of light admits positive, zero and negative values. The state of vanishing deflection angle occurs at different coordinate radii and the value of each radius depends on the behavior of spacetime torsion near the wormhole throat. We therefore observed that, depending on model parameters, the wormhole configuration can act as a converging or diverging lens. It is worth mentioning that, solutions comprising rich information on wormhole configurations in PGT may be found by taking, *i*) a general form of the red-shift function, *ii*) a non-zero spin density of matter distribution, and *iii*) different functionalities of the torsion components. Specially the second case could provide a setting based on which the effects of spin on the geometry of a wormhole configuration can be surveyed. More interestingly, these effects can be helpful in probing the geometrical feature of the spacetime that couples to spin of matter, i.e., the spacetime torsion, via highly sensitive observational instruments. However, regarding these cases, the resultant field equations are too complicated to be solved analytically and more advanced mathematical techniques are needed in order to overcome the problem. Work along this line is currently in progress and the results will be reported as an independent work.

6 Acknowledgements

This work has been supported financially by Research Institute for Astronomy & Astrophysics of Maragha (RIAAM).

References

- [1] C. W. Misner and J. A. Wheeler, Ann. Phys. **2**, 525 (1957);
C. W. Misner, Phys. Rev. **118**, 1110 (1960).
- [2] J. A. Wheeler, Ann. Phys. **2**, 604 (1957);
J. A. Wheeler, Geometrodynamics (Academic, New York, 1962).
- [3] J. A. Wheeler, Phys. Rev. **97**, 511 (1955).
- [4] S. W. Hawking, Phys. Rev. D **37**, 904 (1988).
- [5] R. W. Fuller and J. A. Wheeler, Phys. Rev. **128**, 919 (1962).
- [6] R. P. Geroch, J. Math. Phys. **8**, 782 (1967).
- [7] M. S. Morris and K. S. Thorne, Am. J. Phys. **56**, 395 (1988).
- [8] M. S. Morris, K. S. Thorne and U. Yurtsever, Phys. Rev. Lett. **61**, 1446 (1988).
- [9] M. Visser, *Lorentzian Wormholes: From Einstein to Hawking* (AIP, Woodbury, USA, 1995);
D. Hochberg and M. Visser, Phys. Rev. D **56**, 4745 (1997).
- [10] H. Epstein, V. Glaser and A. Jaffe, IL Nuovo Cimento, **36**, 1016 (1965).
- [11] D. Hochberg, T. W. Kephart, Phys. Lett. B **268**, 377 (1991).
- [12] G. Klinkhammer, Phys. Rev. D **43**, 2542 (1991).

- [13] S. W. Hawking, Phys. Rev. D **46**, 603 (1992);
E. Poisson and M. Visser, Phys. Rev. D **52**, 7318 (1995);
M. Chianese, E. Di Grezia, M. Manfredonia and G. Miele, Eur. Phys. J. Plus **132**, 164 (2017).
- [14] F. S. N. Lobo, Phys. Rev. D **71**, 124022 (2005);
P. K. F. Kuhfittig, Class. Quant. Grav. **23**, 5853 (2006);
F. S. N. Lobo, F. Parsaei and N. Riazi, Phys. Rev. D **87**, 084030 (2013);
Y. Heydarzade, N. Riazi and H. Moradpour, Can. J. Phys. **93**, 1523 (2015).
- [15] V. Folomeev and V. Dzhunushaliev, Phys. Rev. D **89**, 064002 (2014).
- [16] F. S. N. Lobo, Classical and Quantum Gravity Research, 1-78, (2008), Nova Sci. Pub. ISBN 978-1-60456-366-5, arXiv:0710.4474 [gr-qc].
- [17] G. Dotti, J. Oliva, R. Troncoso, Phys. Rev. D **75**, 024002 (2007);
H. Maeda, M. Nozawa, Phys. Rev. D **78**, 024005 (2008);
M. H. Dehghani and Z. Dayyani, Phys. Rev. D **79**, 064010 (2009);
M. R. Mehdizadeh and F. S. N. Lobo, Phys. Rev. D **93**, 124014 (2016).
- [18] H. Moradpour, N. Sadeghnezhad and S. H. Hendi, Can. J. Phys. **95**, 1257 (2017).
- [19] N. M. Garcia and F. S. N. Lobo, Phys. Rev. D **82**, 104018 (2010);
M. Zubair, S. Waheed and Y. Ahmad, Eur. Phys. J. C **76**, 444 (2016).
- [20] A. G. Agnese and M. La Camera, Phys. Rev. D **51**, 2011 (1995);
K. K. Nandi, A. Islam, and J. Evans, Phys. Rev. D **55**, 2497 (1997);
L. A. Anchordoqui, S. P. Bergliaffa, and D. F. Torres, Phys. Rev. D **55**, 5226 (1997);
R. Shaikh and S. Kar, Phys. Rev. D **94**, 024011 (2016).
- [21] N. Furey and A. DeBenedictis, Class. Quantum Grav. **22**, 313 (2005);
F. S. N. Lobo and M. A. Oliveira, Phys. Rev. D **80**, 104012 (2009);
A. De Benedictis, D. Horvat, Gen. Relat. Gravit. **44**, 2711 (2012);
M. Sharif and I. Nawazish, Annals of Physics, **389**, 283 (2018).
- [22] K. A. Bronnikov and A. M. Galiakhmetov, Grav. Cosmol. **21**, 283 (2015);
M. R. Mehdizadeh and A. H. Ziaie, Phys. Rev. D **95**, 064049 (2017);
Phys. Rev. D **99**, 064033 (2019).
- [23] S. H. Mazharimousavi, M. Halilsoy, and Z. Amirabi, Phys. Rev. D **81**, 104002 (2010);
P. Kanti, B. Kleihaus and J. Kunz, Phys. Rev. D **85**, 044007 (2012).
- [24] R. Shaikh, Phys. Rev. D **92**, 024015 (2015);
F. Rahaman, N. Paul, A. Banerjee, S. S. De, S. Ray and A. A. Usmani, Eur. Phys. J. C **76**, 246 (2016);
P. H. R. S. Moraes, P. K. Sahoo, Phys. Rev. D **96**, 044038 (2017);
M. A. G. Richarte, I. G. Salako, J. P. Moraes Graca, H. Moradpour, and A. Ovgun, Phys. Rev. D **96**, 084022 (2017);
K. Jusufi, N. Sarkar, F. Rahaman, A. Banerjee and S. Hansraj, Eur. Phys. J. C **78** 349 (2018).
- [25] C. M. Will, Living Rev. Rel. **17** (2014) 4.
- [26] Virgo and LIGO Scientific collaborations, B. P. Abbott et al., Phys. Rev. Lett. **116**, 061102 (2016).
- [27] The Event Horizon Telescope Collaboration, The Astrophysical Journal Letters, **875**, L1-L6 (2019).

- [28] S. W. Hawking and G. F. R. Ellis, “*The Large Scale Structure of Spacetime*,” Cambridge University Press, Cambridge (1973).
- [29] S. Capozziello and M. De Laurentis, Phys. Rep., **509**, 167 (2011);
A. De Felice and S. Tsujikawa, Living Rev. Rel., **13**, 3 (2010).
- [30] F. W. Hehl, P. Von der Heyde, and G. D. Kerlick and J. M. Nester, Rev. Mod. Phys. **48**, 393 (1976).
- [31] V. De Sabbata and M. Gasperini, “*Introduction to Gravitation*,” World Scientific, Singapore (1986).
- [32] T. W. B. Kibble, J. Math. Phys. **2**, 212 (1961).
- [33] M. Blagojevic, arXiv:gr-qc/0302040.
- [34] Y. N. Obukhov, Int. J. Geom. Meth. Mod. Phys. **3**, 95 (2006).
- [35] Y. N. Obukhov, V. N. Ponomarev, and V. V. Zhytnikov, Gen. Rel. Grav. **21**, 1107 (1989).
- [36] F. W. Hehl, J. D. McCrea, E. W. Mielke, and Y. Ne’eman, Phys. Rep. **258**, 1 (1995).
- [37] M. Blagojevic, “*Gravitation and Gauge Symmetries*,” Institute of Physics, Bristol (2002).
- [38] M. Blagojevic and F. W. Hehl, “*Gauge Theories of Gravitation: A reader with commentaries*,” Imperial College Press, London, (2013).
- [39] A. V. Minkevich, Grav. Cosmol. **12**, 11 (2006);
A. V. Minkevich and A. S. Garkun, Class. Quantum Grav. **23**, 4237 (2006);
A. V. Minkevich, Acta Phys. Pol. B **38**, 61 (2007);
A. V. Minkevich, A. S. Garkun and V. I. Kudin, Class. Quantum Grav. **24**, 5835 (2007);
A. V. Minkevich, Ann. Fond. Louis de Broglie **32**, 253 (2007).
- [40] C. H. LEE, Phys. Lett. B, **130**, 257 (1983).
- [41] J. A. R. Cembranosa, and J. G. Valcarcel, JCAP 01 (2017) 014.
- [42] J. M. Nester, in “*Introduction to Kaluza-Klein Theories*,” edited by H. C. Lee, World Scientific, Singapore (1984).
- [43] F. W. Hehl, in “*Proceedings of the 6th Course of the International School of Cosmology and Gravitation on Spin, Torsion, and Supergravity*,” edited by P. G. Bergmann and V. de Sabatta, Plenum, New York, (1980).
- [44] K. Hayashi and T. Shirafuji, Prog. Theor. Phys., **64**, 866 (1980); **64**, 883 (1980); **64**, 2222 (1980).
- [45] E. W. Mielke, “*Geometrodynamics of Gauge Fields*, Akademie-Verlag, Berlin (1987).
- [46] F. Gronwald and F. w. Hehl, in “*Proceedings of the 14th Course of the School of Gravitation and Cosmology (Erice)*,” edited by P. G. Bergmann, V. de Sabatta and H. J. Treder, World Scientific, Singapore (1996).
- [47] F. W. Hehl, Y. Ne’eman, J. Nitsch and P. Von Der Heyde, Phys. Lett. B, **78**, 102 (1987).
- [48] E. Sezgin and P. van Nieuwenhuizen, Phys. Rev. D **21**, 3269 (1980).
- [49] M. Blagojevic and I. A. Nikolic, Phys. Rev. D **28**, 2455 (1983);
I. A. Nikolic, Phys. Rev. D **28**, 2508 (1984).

- [50] H. J. Yo and J. M. Nester, Int. J. Mod. Phys. D **8**, 459 (1999).
- [51] H. Chen, J. M. Nester, and H. J. Yo, Acta Phys. Pol. B **29**, 961 (1998).
- [52] R. Hecht, J. M. Nester, and V. V. Zhytnikov, Phys. Lett. A **222**, 37 (1996).
- [53] H. J. Yo and J. M. Nester, Int. J. Mod. Phys. D **8**, 459 (1999).
- [54] H.-J. Yo, and J. M. Nester, Mod. Phys. Lett. A **22**, 2057 (2007).
- [55] K. F. Shie, J. M. Nester, and H. J. Yo, Phys. Rev. D **78**, 023522 (2008).
- [56] H. Chen, F.-H. Ho, J. M. Nester, C.-H. Wang and H.-J. Yo, JCAP 0910:027 (2009).
- [57] P. Baekler, F. W. Hehl and J. M. Nester, Phys. Rev. D **83**, 024001 (2011).
- [58] F. S. N. Lobo (Editor), “ *Wormholes, Warp Drives and Energy Conditions*,” Springer (2017).
- [59] S. M. Carroll, M. Hoffman, and M. Trodden, Phys. Rev. D **68**, 023509 (2003);
Z.-K Guo, Y.-S. Piao and Y.-Z. Zhang, Phys. Lett. B **594**, 247 (2004); E. Elizalde, S. Nojiri, and
S. D. Odintsov, Phys. Rev. D **70** 043539 (2004); J.-gang Hao and X.-zhou Li, Phys. Rev. D **70**
043529 (2004);
V. Faraoni, Class. Quant. Grav., **22**, 3235 (2006);
H. Moradpour, R. C. Nunes, E. M. C. Abreu and J. A. Neto, Mod. Phys. Lett. A **32**, 1750078
(2017);
H. Moradpour, S. A. Moosavi, I. P. Lobo, J. P. Morais Graca, A. Jawad and I. G. Salako, Eur.
Phys. J. C, **78**, 829 (2018).
- [60] S. Weinberg, “*Gravitation and cosmology: principles and applications of the general theory of relativity*,” Wiley (1972).
- [61] W. Hasse and V. Perlick, Gen. Relativ. Gravit. **34**, 415 (2002).
- [62] V. Perlick, Living Rev. Relativity, **7**, 9 (2004).
- [63] R. Shaikh, P. Banerjee, S. Paul and T. Sarkar, Phys. Lett. B **789**, 270 (2019).
- [64] M. Silvia and R. Esteban, “*Gravitational Lensing And Microlensing*,” World Scientific (2002);
F. Courbin and D. Minniti, (Eds.), “*Gravitational Lensing: An Astrophysical Tool*,” Springer
(2008);
M. Kilbinger, Rep. Prog. Phys. **78**, 086901 (2015);
S. Dodelson, “*Gravitational Lensing*,” Cambridge University Press (2017);
S. E. Gralla, D. E. Holz and Robert M. Wald, arXiv:1906.00873 [astro-ph.HE].
- [65] K. S. Virbhadra, D. Narasimha, and S. M. Chitre, Astron. Astrophys. **337**, 1 (1998);
K. S. Virbhadra and G. F. R. Ellis, Phys. Rev. D **65**, 103004 (2002).
- [66] T. Treu, Annu. Rev. Astron. Astrophys. **48**, 87 (2010);
T. Treu, P. J. Marshall and D. Clowe, Am. J. Phys. **80**, 753 (2012);
F. De Paolis, M. Giordano, G. Ingrosso, L. Manni, A. Nucita, and F. Strafella, Universe **6**, 2
(2016).
- [67] T. Muller, Phys. Rev. D **77**, 044043 (2008).
- [68] T. Harko, Z. Kovacs, and F. Lobo, Phys. Rev. D **78**, 084005 (2008);
C. Bambi, Phys. Rev. D **87**, 084039 (2013).

- [69] V. Cardoso, E. Franzin and P. Pani, Phys. Rev. Lett. **116**, 171101 (2016);
V. Cardoso, S. Hopper, C. F. B. Macedo, C. Palenzuela, and P. Pani, Phys. Rev. D **94**, 084031 (2016);
S. Aneesh, S. Bose, and S. Kar, Phys. Rev. D **97**, 124004 (2018).
- [70] C. Bambi, Phys. Rev. D **87**, 107501 (2013).
- [71] P. G. Nedkova, V. K. Tinchev, and S. S. Yazadjiev, Phys. Rev. D **88**, 124019 (2013);
A. Abdujabbarov, B. Juraev, B. Ahmedov and Z. Stuchlik, Astrophys. Space Sci. **361**, 226 (2016);
R. Shaikh, Phys. Rev. D **98**, 024044 (2018);
G. Gyulchev, P. Nedkova, V. Tinchev and S Yazadjiev, **78**, 544 (2018);
R. Shaikh, Phys. Rev. D **98**, 024044 (2018).
- [72] M. Amir, A. Banerjee and S. D. Maharaj, Annals of Phys. **400**, 198 (2019).
- [73] T. Ohgami and N. Sakai, Phys. Rev. D **91**, 124020 (2015).
- [74] H. Falcke, F. Melia, and E. Agol, Astrophys. J. **528**, L13 (2000).
- [75] A. Grenzebach, “ The Shadow of Black Holes: An Analytic Description,” Springer (2016);
P. V. P. Cunha and C. A. R. Herdeiro, Gen. Relativ. Gravit. **50**, 42 (2018).